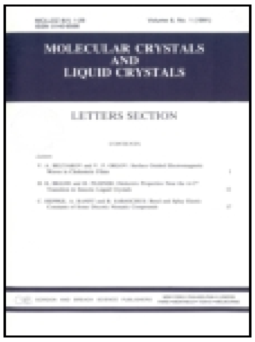

Molecular Crystals and Liquid Crystals

ISSN: 1542-1406 (Print) 1563-5287 (Online) Journal homepage: http://www.tandfonline.com/loi/gmcl20

Effects of boundary and bulk control technology in cholesteric liquid crystals

Gi Heon Kim, Won-Jae Lee, Han Na Kim & Yong-Hae Kim

To cite this article: Gi Heon Kim, Won-Jae Lee, Han Na Kim & Yong-Hae Kim (2016) Effects of boundary and bulk control technology in cholesteric liquid crystals, Molecular Crystals and Liquid Crystals, 633:1, 72-79, DOI: 10.1080/15421406.2016.1177886

To link to this article: http://dx.doi.org/10.1080/15421406.2016.1177886

MOLECULAR CRYSTALS AND LIQUID CRYSTALS
2016, VOL. 633, 72–79
http://dx.doi.org/10.1080/15421406.2016.1177886

Effects of boundary and bulk control technology in cholesteric liquid crystals

Gi Heon Kim, Won-Jae Lee, Han Na Kim, and Yong-Hae Kim

Smart I/O Platform Research Department, Electronics and Telecommunications Research Institute, Yuseong-Gu, Daejeon, Korea

ABSTRACT

We fabricate a cholesteric liquid crystal display (Ch-LCD) having high reflectance and fast response time by doping R-811 into a nematic LC. The field-on and the field-off response times are 39 and 15 ms, respectively. The helical pitch is governed by R-811 that induced the cholesteric color. The boundary and bulk condition are strong effect on changes in the electro-optic behavior. The boundary condition controlled by rubbing strength has strong effects on the field-off response time and the reflectance variation. The bulk condition controlled by cell gap and R-811 concentration induced significant changes on operating voltage and threshold voltage.

KEYWORDS

Cell gap; cholesteric liquid crystal; driving voltage; response time; rubbing

Introduction

Cholesteric liquid crystal displays (Ch-LCDs) have been extensively investigated because of its electrical (low power consumption and molecular orientation memory), optical (high reflectance and outdoor readability), physical (light weight, thinner thickness) and special (self-assembling periodic helical structure) properties [1–10]. The Ch-LC display opens many opportunities from small displays for electronic books and navigator to large signage displays. The Ch-LCDs are fabricated by mean of doping some chiral agent into a nematic liquid crystal (NLC), which shows full color capability without color controlling elements or color filter [11, 12]. The Ch-LCD has stacked structure that changes to the different phase when a driving voltage is applied.

The Ch-LC phase has a unique feature of reflecting incident visible light selectively, which is dependent on twisted direction of helical pitch and helical pitch length. Concentration of added chiral dopant into NLC caused an appreciable change on the color variation that is determined by the selective Bragg reflection condition [13, 14]. The average refractive index of the NLC or HTP (helical twisting power) of the chiral dopant induces the cholesteric color change. This reflected color has been a topic of consideration scientific and practical interest because of its potential applications in display, which needs to be controlled.

The cholesteric color can be controlled by means of temperature [15, 16] and electric field [17]. It is well known that the helical pitch of the Ch-LC molecules is influenced by thermodynamic behavior; however, color changes in the Ch-LC phase do not occur in many Ch-LC

CONTACT Gi Heon Kim kimgh411@etri.re.kr Smart I/O Platform Research Department, Electronics and Telecommunications Research Institute, 161 Gajeong-Dong, Yuseong-Gu, Daejeon 305-700, Korea.

Color versions of one or more of the figures in the article can be found online at www.tandfonline.com/gmcl.

mixtures with increasing temperature. The sensitivity of the helical pitch to external electric fields has made the Ch-LC mixtures an attractive material as switchable reflector, display and polarization elements. However, the electro-optic issues of high turn-on voltage, slow response time and short-term stability/reliability are still challenges.

To obtain low driving voltage and fast response time for the practical display applications, this study focused on changing the reflective color and reflectance at the interfacial and the bulk state. The conventional Ch-LC molecule with homogenous alignment (where the helical orientation is perpendicular to the substrate) is fixed at the surface with strong anchoring force. Therefore, the boundary and the bulk characteristics of Ch-LC devices are strong effect on changes in the optical and the electro-optic behavior.

Experimental

Materials

The right-handed Ch-LC materials were prepared by doping a chiral agent (R-811) into NLC. Here, 4-(hexyloxy) benzoic acid 4-[[[(1R)-1-methylheptyl]oxy]carbonyl]phenyl ester (R-811) was supplied from Merck Co. Ltd. The chemical structure of R-811 is shown in Fig. 1. MLC-6657-000 (MLC-6657) as an NLC was supplied from Merck Co. Ltd.

Dielectric anisotropy (dE) of MLC-6657 (T_{NI}, 95.6°C) is 32.9, and extraordinary and ordinary refractive indices are 1.6766 and 1.5065, respectively. Extraordinary and ordinary dielectric indices are 40.0 and 7.1, respectively. The Ch-LC mixture was stirred at 100°C (cleaning point of MLC-6657) for 12 h to dissolve. The Ch-LC mixtures were prepared, whose compositions and weight ratio are listed in Table 1. An alignment layer (SE-5291) for homogenous orientation of the Ch-LC molecules was purchased from Nissan Chemical Industries Co. Ltd. SE-5291 is a preimidized type of alignment coating.

The cholesteric-isotropic phase transition temperature ($T_{Ch\text{-}I}$) was decreased with decreasing chiral pitch length [15]. The Ch-LC molecules having a relatively short chiral pitch easily moved to the isotropic state with increasing temperature.

Formation of Ch-LC devices

For analyzing characteristics of the Ch-LC molecules, a plastic-based device was fabricated. The cell is composed of sandwiched plastic substrates with indium zinc oxide (IZO) electrode and Ch-LC layer. Transparent IZO electrode coated onto polycarbonate (PC) film is defined by a conventional photolithography technique.

The preimidized SE-5291 was spin-coated, and the obtained film was subsequently heated at 90°C for 20 min to evaporate solvent and then imidized at 180°C for 1 h. The obtained PI film (thickness, 120 nm) was rubbed. Rubbing of the PI film was performed by rotational motion of fibrous machine [18]. The cylinder covered with rayon (pile density, 53,000 ea cm^{-2}) was rotated at a constant speed (n) of 1000 rpm, while the PI-coated substrate is moved

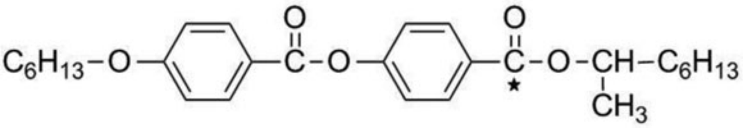

Figure 1. Chemical structure of R-811 used in this study.

Table 1. Compositions of weight ratio of Ch-LC mixtures.

Sample	Compositions	Weight Rratio (wt%)	$T_{Ch\text{-}I}$(°C)	λ_{max} (nm)
1	R811/MLC-6657	22/78	67	625
2	R811/MLC-6657	24/76	–	585
3	R811/MLC-6657	26/74	58	535
4	R811/MLC-6657	29/71	–	485
5	R811/MLC-6657	32/68	48	460
6	R811/MLC-6657	36/64	–	425

with a constant translating speed (ν) of 1200 mm s^{-1} under a rotational cylinder. The total length of rubbing cloth (L (mm)) in contact with the PI film is expressed as follows:

$$L = Nl\left(\frac{1+2n\pi}{60\upsilon}\right),$$

where r is radius of rotational cylinder, N is cumulative number of movement of the rubbing table and l is the contact length between the rotational cylinder and the PI film. In this study, rubbing strength (RS) is defined to be the same as the calculated total length of rubbing cloth (L). We changed l to obtain varying orientation degree of the PI molecule chains.

The Ch-LC cell (Fig. 2) was assembled using pairs of the substrates thus prepared with their rubbing directions antiparallel [19]. The gap of the devices was controlled by using a 2.5, 4, 10 and 20 μm thick ball spacer. The Ch-LC mixture was introduced into sandwiched plastic substrate by mean of modified ODF (one drop fill) method at room temperature. After injecting the Ch-LC mixture, the cell heated to 90°C (isotropic phase) and then cooled slowly down to room temperature to obtain a stabilized planar phase.

Characterization

The PI film thickness was measured using a Tencor Instrument Alpha-Step 500. The reflective light intensity is analyzed by using spectrophotometer (Otsuka MCPD-3700) with a standard D65 incident light at 0 degree. Electro-optic characteristics of the Ch-LCDs were studied with Otsuka FPD-5200 system. Halogen lamp was used as a light source. We defined 100% reflectance as reflectance of the probe light through an empty cell without Ch-LC mixture on mirror.

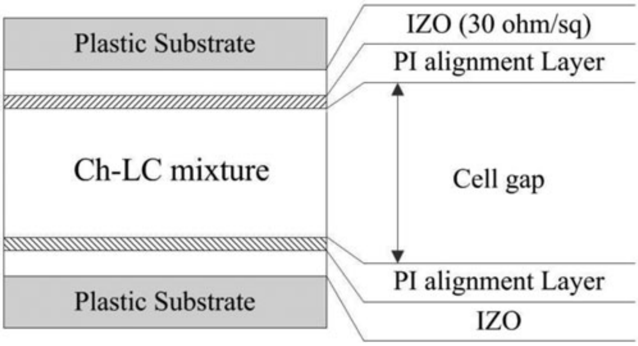

Figure 2. A cross-section of the Ch-LC device used for evaluation of electro-optic (EO) behavior.

Results and discussion

Effects of chiral agents

The aligned Ch-LC molecules in a fixed cell gap are forming a helically twisted structure. In the cholesteric phase (planar state) without an electric field, its helical axis is normal to the plastic substrate, a specific wavelength of incident visible light is reflected by the periodically differing refractive index in the Ch-LC phase [20]. The twisted Ch-LC in the planar state shows a specific color that is mainly dependent on the chiral pitch number, birefringence and wavelength of incident light [1]. With increasing applied electric field, the orientation of the Ch-LC molecules is changed along the director of the electric field, and finally reached a transparent state (homeotropic state).

Figure 3 shows the selective reflectance variation of the Ch-LC mixtures depending on the content of R-811. The reflective wavelength of 22/78 (R-811/MLC-6657) showed a maximum value of reflectance at 625 nm and shifted to a short wavelength to 425 nm with increasing added content of R-811 [21]. The wavelength variation is strongly influenced by solubility of R-811. As shown in Fig. 3, the increased R-811 content decreases pitch length, however, which is not responsible for the maximum reflective value change. These results indicate that the selective reflectance mainly induced by the chiral pitch in interface region between the Ch-LC phase and the rubbed PI alignment layer, but is not due to the overall chiral pitch in the bulk region. With decreasing the chiral pitch length by adding R-811, the reflective wavelength moved to blue color and wavelength width becomes narrow.

Effects of rubbing strength

In order to investigate effects of rubbing strength on electrical and optical properties of the Ch-LC devices, we prepared five 22/78 Ch-LC devices with differing rubbing strength. The chiral pitch of the Ch-LC is dependent on the boundary effects between the Ch-LC molecules and the PI layer, and the boundary condition at interface hinders continuous reduction of the chiral pitch [15]. Rubbing strength (mm) is responsible for interfacial interaction between

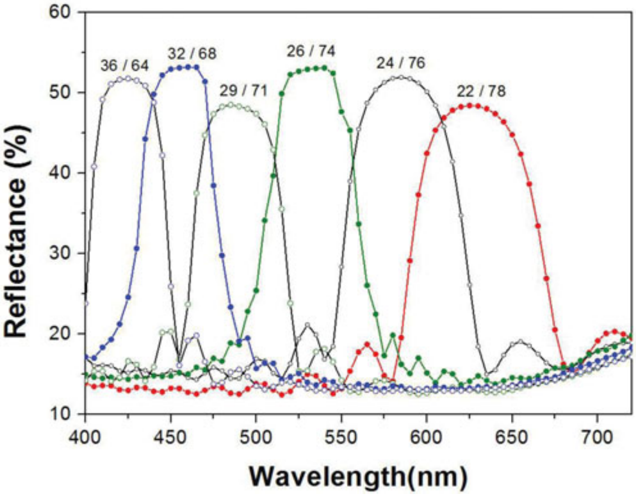

Figure 3. The reflectance spectrum of the Ch-LCDs (cell gap, 4 μm) with different R-811/MLC-6657 mixtures.

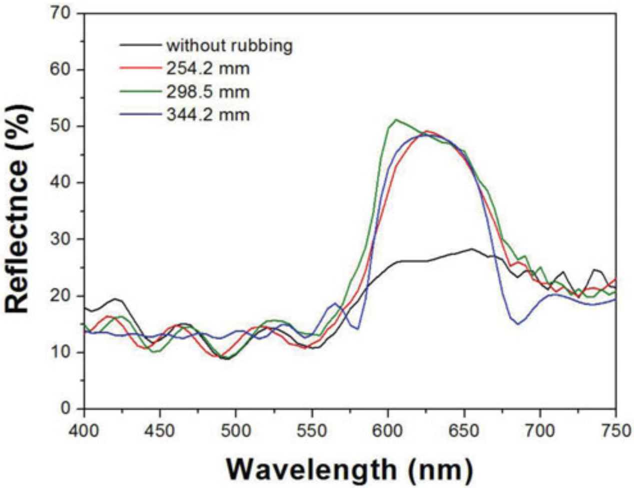

Figure 4. The effect of rubbing strength on the reflectance spectrum of the Ch-LCDs (cell gap, 4 μm) with 22/78 mixture.

Ch-LC molecules and the rubbed PI film. Fig. 4 shows the effect of the rubbing strength on reflectance spectrum of the Ch-LCDs with 22/78 mixture.

Reflectance at 625 nm increases with increasing rubbing strength. This is consistent with the established rubbing mechanism in which the LC molecules become aligned to the rubbing direction with increasing the rubbing strength [18]. The Ch-LC molecules on the unrubbed PI surface showed randomly distributed, resulting in low reflectance due to light scattering as shown in Fig. 4. When the rubbing strength exceeds 254 mm, width and intensity of the selective reflective spectrum do not show a quantitative trend with the rubbing strength.

Figure 5 shows the measured reflectance versus the applied AC voltage (30 Hz) of the 4 μm thick Ch-LC device. The reflectance of the Ch-LC devices is decreased with the electric field as shown in Fig. 5. It is observed that with increasing AC voltage, the reflectance remained hardly changed until ~3 V and then it decreased steeply. This behavior results from changes of the cholesteric phase from planar state to focal conic state, and eventually reached homeotropic

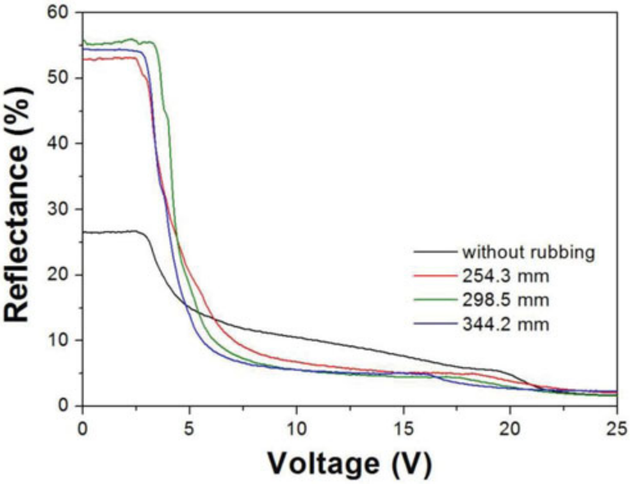

Figure 5. The effect of rubbing strength on the electro-optical response of the Ch-LC devices (cell gap, 2.5 μm) with 22/78 mixture. The maximum reflectance is adjusted to be 100%.

Table 2. Electro-optic performance of the Ch-LCD with 22/78 mixture driven by an AC bias voltage (30 Hz) of 25 V as a function of rubbing strength.

	Rubbing strength (mm)	Response time (ms) (T_r/T_f)	Contrast ratio
1	0	38.6/41.2	19.7:1
2	254.3	38.5/31.5	31.2:1
3	298.5	38.4/19.6	42.5:1
4	344.2	39.0/15.1	41.4:1

state at above 24 V, which is affected by PI thickness, cell gap, R-811 content and the chiral pitch. The applied electrical strength is much higher than that of a normal NLC device because the Ch-LC phases have stable planar and focal conic states.

The maximum contrast ratio on the rubbed cell is approximately 43, however, which decreases to 20 on the cell without rubbing process. The unrubbed PI alignment layer impedes the orientation and ordering of Ch-LC molecules, therefore, the unrubbed Ch-LC device shows a relatively low reflectance of 27%. In order to explore the effect of rubbing strength on optical switching speed of the Ch-LCDs, we next investigated response times of the cells (Table 2). As shown in Table 2, the field-on response time is not changed within experimental range, although the rubbing strength influenced the ordering and orientation of Ch-LC molecules.

The helical pitch is maintained by the anchoring force that is not influenced by the rubbing strength. The boundary condition at interface between the Ch-LC molecules and the PI alignment layer is unlikely to have caused any appreciable difference in the turn-on switching behavior. The applied electric torque changes orientation of the twisted LC molecules, such that the device becomes transparent. The field-on response time T_r (field-off response time T_f) is the time taken for the reflectance to change from 90% to 10% by an electric field. The response times (T_r and T_f) depends on cell gap d, pitch P, viscosity η_1, applied voltage E and effective elastic constant K_{eff} as follows [19, 22]:

$$
\begin{aligned}
V_{th} &= \frac{d\pi^2}{P}\sqrt{\frac{k_{eff}}{\varepsilon_0\,|\Delta\varepsilon|}} \\
T_r &= \frac{\eta_1}{\varepsilon(abs(\Delta\varepsilon))E^2 - K_{22}\pi/2d^2} \\
T_f &= \frac{\eta_1 P^2}{\pi k_{eff}}
\end{aligned}
\tag{1}
$$

The field-off response time gradually decreased until 15 ms. The response time of on/off operation on the Ch-LC device with rubbing strength of 344.2 mm is about 54.1 ms. When the applied voltage is ceased, the field-off response time is strongly influenced by the boundary condition, which is dependent on the chiral pitch length, cell gap, rubbing strength, charged mobile impurities in LC phase and azimuthal anchoring energy (AAE) [19]. The rubbing strength influences AAE that is responsible for the response time of off operation.

Effects of cell gap

Cell gap of LCD largely influences the optical switching behavior by Eq. (1). We fabricated the four Ch-LC devices with varying cell gap to verify effects of chiral pitch number. Fig. 6 shows the changes of reflectance on the green Ch-LC device having 26/74 mixture with increasing

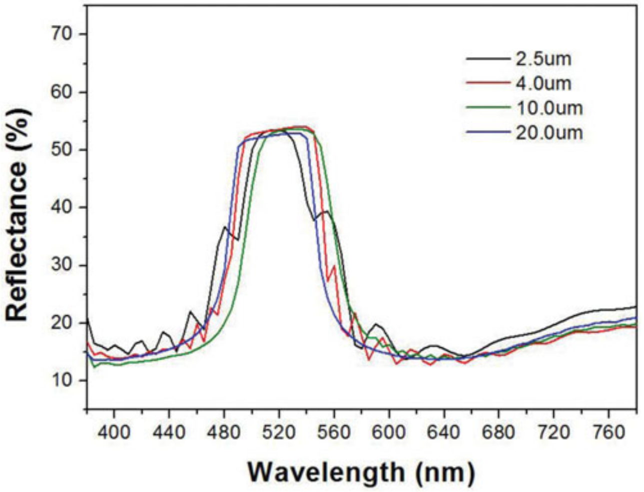

Figure 6. The effect of cell gap on the reflectance spectrum of the Ch-LCDs with 26/74 mixture.

cell gap (2.5, 4.0, 10 and 20 μm). Even though the chiral pitch number increased with increasing cell gap, however, the reflectance mainly induces by the pitch length at the interface region as previously stated. This result indicates that optical behavior of the Ch-LC devices such as wavelength and wavelength width of the reflective light is independent of the cell gap.

Figure 7 shows the curves of reflectance versus applied AC voltage (30 Hz) of the Ch-LC devices with 22/78 mixture as a function of cell gap. The phase transition voltage from cholesteric phase to homeotropic phase of 2.5 μm thick device was about 24 V, however, that of 20 μm thick device was above 50 V. The 2.5 μm thick device leads to reduction in driving and turn-on operational voltage. The reduction in driving voltage is believed to be achieved by decreasing the cell gap. This high operating voltage is thought to be induced by the increased steric hindrance and intermolecular interaction that is caused by the increased chiral pitch number. The R-811 content has a strong effect on the reflective color variation and turn-on

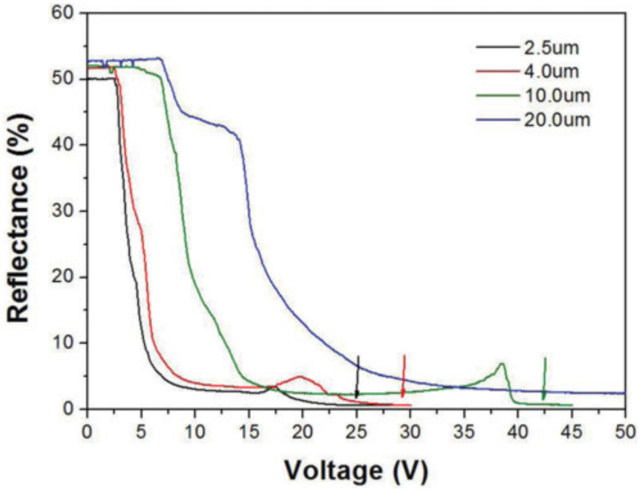

Figure 7. Dependence of the cell gap on the reflectance versus AC voltage curves of the Ch-LC devices with 22/78 mixture.

driving voltage. Hwang et al. reported that the reduction in turn-on voltage can be obtained by the adding of the high birefringence and dielectric anisotropic dopant [5].

Conclusions

The Ch-LC mixtures having a low driving voltage and high reflectance has been demonstrated with R-811 having a relatively low helical twisting power in MLC-6657. The aligned Ch-LC director is fixed with infinite anchoring force on the PI surface, which induced the initial optical image of the Ch-LC device. This boundary condition at the interface between MLC-6657 and the PI alignment layer is not caused any appreciable changes in the planar-homeotropic phase transition switching speed when the applied voltage is turned on. However, the relaxation of the Ch-LC molecules when the applied voltage is turned off is strongly influenced by the boundary condition. The CL-LC material shows a relatively fast optical response time (T_r/T_f, 39.0/15.1 ms), however, a few milliseconds is required for updating moving pictures. The contrast ratio is approximately 42, which is dependent on the boundary condition.

The reflectance and the reflective wavelength are influenced by the chiral pitch in the interfacial region and the solubility of R-811 in the bulk region. The reduction in applied voltage can be achieved by the decreased cell gap and R-811 content. The driving and the turn-on voltage are influenced by the bulk properties on the Ch-LC device. The reduction in the optical switching speed and the driving voltage is believed to be obtained by decreasing chiral dopant content and cell gap, and adding chiral dopant having high helical twisting power.

Funding

This research was funded by the MSIP (Ministry of Science, ICT & Future Planning), Korea in the ICT R&D Program (The core technology development of light and space adaptable energy-saving I/O (input/output) platform for the future advertising service).

References

[1] Lee, H. H., Kim, J., Yi, J., Yamamoto, S., & Kikuchi, H. (2009). *J. Applied Phys.*, *106*, 014503(1)-014503(5).
[2] Kim, Y., Wada, M., & Tamaoki, N. (2014). *J. Mater. Chem. C*, *2*, 1921–1926.
[3] Roohnikan, M., Ebrahimi, M., Ghaffarian, S. R., & Tamaoki, N. (2013). *Liq. Cryst.*, *40*, 314–320.
[4] Roy, D. et al. (2014). *J. Chem. Phys.*, *140*, 074502(1)-074502(6).
[5] Hwang, J. Y., Kang, Y., Bae, K., Yu, C., & Kim, J. (2012). *IMID 2012 Digest*, 380–381.
[6] Serbina, M. I., Kasian, N. A., & Lisetski, L. N. (2013). *Liq. Cryst.*, *58*, 155–159.
[7] Hayashi, H., Wang, A., Kawabata, K., & Goto, H. (2013). *Mater. Chem. Phys.*, *137*, 816–824.
[8] Timirov, Y. I., Skaldin, O. A., & Gareeva, E. R. (2013). *Tech. Phys. Lett.*, *39*, 116–119.
[9] Hsu, W., Ma, J., Myhre, G., Balakrishnan, K., & Pau, S. (2013). *J. Opt. Soc. Am. A*, *30*, 252–258.
[10] Wang, C., & Lin, T. (2012). *J. Display Tech.*, *8*, 613–616.
[11] Wang, X., Liu, D., Li, W., Tian, Q., & Zhou, X. (2013). *Mol. Cryst. Liq. Cryst.*, *571*, 57–66.
[12] Wa, W. H. J., Myhre, G., Balakrishnan, K., & Pau, S. (2013). *J. Opt. Soc. Am. A*, *30*, 252–258.
[13] Wang, C. T., & Lin, T. H. (2012). *J. Display Technol.*, *8*, 613–616.
[14] Cheng, K. T., & Li, J. H. (2009). *SID 09 Digest*, *P-135*, 1627–1629.
[15] Bae, K. S. et al. (2010). *SID 10 Digest*, *P-131*, 1755–1757.
[16] Wang, C., Jao, H., & Lin, L. (2012). *SID 12 Digest*, *P-84*, 1379–1381.
[17] Inoue, Y. et al. (2010). *Mol. Liq. Cryst. Liq.*, *516*, 182–189.
[18] Kato, T., Kurosaki, Y., Kiyota, Y., Tomita, J., & Yoshihara, T. (2010). *SID 10 Digest*, *40.2*, 568–571.
[19] Kim, G. H., & Lee,W. J. (2013). *Trans. Mat. Res. Soc. Jpn.*, *38*, 287–290.
[20] Yeon, J., Lee, J., Yoon, J., Park, J., & Kang, D. (2010). *SID 10 Digest*, *56.2*, 838–841.
[21] Braganza, C. et al. (2011). *SID 11 Digest*, *30.2*, 396–399.
[22] Huang, C. Y., Chin, Y. S., & Ke, S.W. (2007). *Appl. Phys. B*, *B86*, 123–127.